Activated protein C targets CD8+ dendritic cells to reduce the mortality of endotoxemia in mice

Edward Kerschen,[1] Irene Hernandez,[1] Mark Zogg,[1] Shuang Jia,[2] Martin J. Hessner,[2] Jose A. Fernandez,[3] John H. Griffin,[3] Claudia S. Huettner,[4] Francis J. Castellino,[5] and Hartmut Weiler[1]

[1]Blood Research Institute, BloodCenter of Wisconsin, Milwaukee, Wisconsin, USA. [2]The Max McGee National Research Center for Juvenile Diabetes, Department of Pediatrics at the Medical College of Wisconsin and the Children's Research Institute of the Children's Hospital of Wisconsin, Milwaukee, Wisconsin, USA. [3]Department of Molecular and Experimental Medicine, The Scripps Research Institute, La Jolla, California, USA. [4]Belfer Institute for Applied Cancer Science, Dana-Farber Cancer Institute, Boston, Massachusetts, USA. [5]Center for Transgene Research, University of Notre Dame du Lac, Notre Dame, Indiana, USA.

Activated protein C (aPC) therapy reduces mortality in adult patients with severe sepsis. In mouse endotoxemia and sepsis models, mortality reduction requires the cell signaling function of aPC, mediated through protease-activated receptor–1 (PAR1) and endothelial protein C receptor (EPCR; also known as Procr). Candidate cellular targets of aPC include vascular endothelial cells and leukocytes. Here, we show that expression of EPCR and PAR1 on hematopoietic cells is required in mice for an aPC variant that mediates full cell signaling activity but only minimal anticoagulant function (5A-aPC) to reduce the mortality of endotoxemia. Expression of EPCR in mature murine immune cells was limited to a subset of $CD8^+$ conventional dendritic cells. Adoptive transfer of splenic $CD11c^{hi}PDCA\text{-}1^-$ dendritic cells from wild-type mice into animals with hematopoietic EPCR deficiency restored the therapeutic efficacy of aPC, whereas transfer of EPCR-deficient $CD11c^{hi}$ dendritic cells or wild-type $CD11c^{hi}$ dendritic cells depleted of $EPCR^+$ cells did not. In addition, 5A-aPC inhibited the inflammatory response of conventional dendritic cells independent of EPCR and suppressed IFN-γ production by natural killer–like dendritic cells. These data reveal an essential role for EPCR and PAR1 on hematopoietic cells, identify EPCR-expressing dendritic immune cells as a critical target of aPC therapy, and document EPCR-independent antiinflammatory effects of aPC on innate immune cells.

Introduction

The recombinant form of human activated protein C (aPC) is used in clinical practice to treat patients suffering from the most severe forms of sepsis. Proposed aPC candidate mechanisms relevant to sepsis therapy include anticoagulation and enhancement of fibrinolysis, antiinflammatory and antiapoptotic effects on endothelial cells and leukocytes, and preservation of endothelial permeability barrier function (1). These biological activities of aPC may be mechanistically grouped into two categories, i.e., (a) enzyme-substrate interactions of soluble aPC with coagulation factors Va and VIIIa and the inhibitor of fibrinolysis plasminogen activator inhibitor–1 (PAI-1), which form the basis of aPC's anticoagulant and profibrinolytic effects; and (b) cell signaling mechanisms initiated by binding of aPC to its receptor, endothelial cell protein C receptor (EPCR, encoded by *Procr*), and subsequent proteolytic activation of the G protein–coupled thrombin receptor PAR1 by the EPCR-aPC complex. More recent data further suggest that aPC may inhibit the proinflammatory activation of TLRs by histones released from dying cells, secondary to the proteolytic degradation of histones by aPC (2)

In mouse models of endotoxemia and sepsis, the cell signaling function of aPC, exerted via proteolytic activation of PAR1 by the aPC-EPCR complex, is a necessary mechanism by which aPC reduces mortality after bacterial infection or after challenge with lethal doses of the TLR4 agonist LPS. This conclusion is based on the observations that therapeutic efficacy of aPC requires its intact proteolytic activity and normal expression of the receptors EPCR and PAR1, and that recombinant variants of aPC with normal anticoagulant activity but greatly diminished cell signaling function (E149A-aPC) fail to improve sepsis outcome in mouse models; whereas an aPC variant with intact cell signaling activity but only minimal anticoagulant function (5A-aPC) appears to be as effective as normal aPC in reducing sepsis mortality (3, 4).

Candidate cellular targets on which aPC-triggered cell signaling must occur to reduce inflammation and sepsis mortality include vascular endothelial cells and leukocytes. Vascular effects of aPC, mediated by engagement of endothelial cell–associated EPCR, are well documented: infusion of aPC attenuates the inflammation-induced loss of endothelial permeability barrier function (5), reduces NO-mediated hypotension (6), and modulates tumor cell extravasation (7). These vasoactive effects of aPC may alleviate inflammation-induced loss of blood pressure and reduce tissue damage secondary to microvascular leakage and edema. Blood pressure–stabilizing effects of aPC have also been documented in critically ill septic patients (8) and in one of two studies in LPS-treated healthy volunteers (9, 10). The protective effects of therapeutic, as well as endogenous, aPC on in vivo vascular barrier function and lethality have been confirmed in LPS-challenged mice (4, 5, 11). In addition, aPC alters gene expression in cultured endothelial cells to promote cell survival, suppresses cytokine-induced upregulation of

Conflict of interest: John H. Griffin serves on the Scientific Advisory Board of Socratech LLC.

Citation for this article: *J Clin Invest.* 2010;120(9):3167–3178. doi:10.1172/JCI42629.

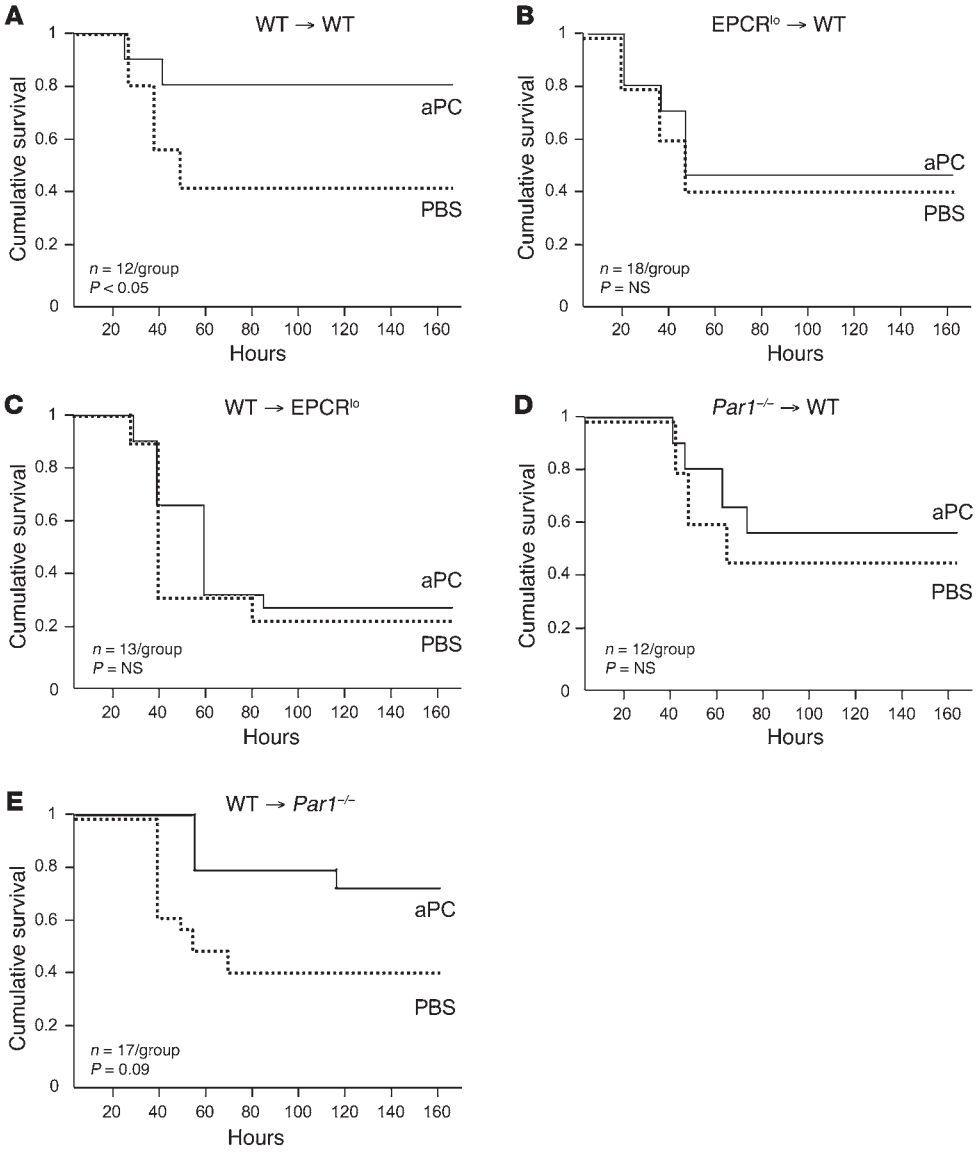

Figure 1
Mortality reduction by aPC requires EPCR and PAR1 expression in BM-derived cells. BM chimeras were generated by reciprocal BM transfers between CD45 isotype–mismatched animals of the indicated genotypes (EPCR^{lo}: reduced EPCR expression; *Par1*$^{-/-}$: PAR1-knockout mice). Eight to 10 weeks after documented hematopoietic reconstitution, animals received a dose of LPS causing 50% mortality in wild-type mice, followed by intravenous infusion of a 10-μg bolus of murine recombinant 5A-aPC (aPC) in PBS or carrier alone. (**A**) BM transfer between wild-type mice does not alter the sensitivity to LPS and response to aPC therapy. Full efficacy of mortality reduction by 5A-aPC requires normal expression of EPCR and PAR1 in hematopoietic cells (**B** and **D**), as well as in non-hematopoietic cells (**C** and **E**). Significance of the aPC effect on 7-day survival was determined by Kaplan-Meier log-rank test.

adhesion molecules mediating leukocyte adhesion, inhibits NF-κB transcriptional networks, and diminishes the expression of inflammatory cytokines and chemokines. Such direct antiinflammatory effects on endothelial cells may contribute to the beneficial effect of aPC therapy on accumulation of neutrophils into the lungs of septic patients prone to pulmonary failure (12, 13).

Data on antiinflammatory effects of aPC on leukocytes are largely derived from in vitro experiments on human immune cells, where EPCR expression has been reported in primary neutrophils (14), monocytes and macrophages (15–17), eosinophils (18), and NK cells (19). Such studies indicate that aPC, predominantly in an EPCR-dependent manner, modulates the inflammatory LPS response of mononuclear leukocytes, reduces leukocyte apoptosis, inhibits leukocyte responses to chemotactic signals (reviewed in refs. 1 and 19), and suppresses inflammatory Wnt5a signaling in human macrophages (17). In contrast, EPCR expression in mice appears to be limited to HSCs with long-term repopulation capacity and as-yet-undefined other cells resident in the BM (20, 21). To the best of our knowledge, no data are available to suggest expression of EPCR on mature murine immune cells. Consistent with this limited expression pattern of EPCR in mouse hematopoietic cells, neither the anticoagulant nor the antiinflammatory activity of endogenous aPC was altered in mice lacking EPCR expression on BM-derived immune cells (22).

Such observations suggest that the mortality-reducing, EPCR-dependent signaling effects of aPC documented in mice could in theory almost exclusively be accounted for by engagement of EPCR on vascular endothelial cells. In a broader context, this raises the question to what extent the various effects of aPC reported for human immune cells correlate with of the mechanisms by which aPC reduces mortality in murine sepsis models. We therefore investigated the role of EPCR expression in BM-derived murine immune cell populations for the therapeutic efficacy of aPC in LPS-induced endotoxemia.

Results

EPCR and PAR1 expression on BM-derived cells is required for the therapeutic efficacy of recombinant 5A-aPC. We first determined the impor-

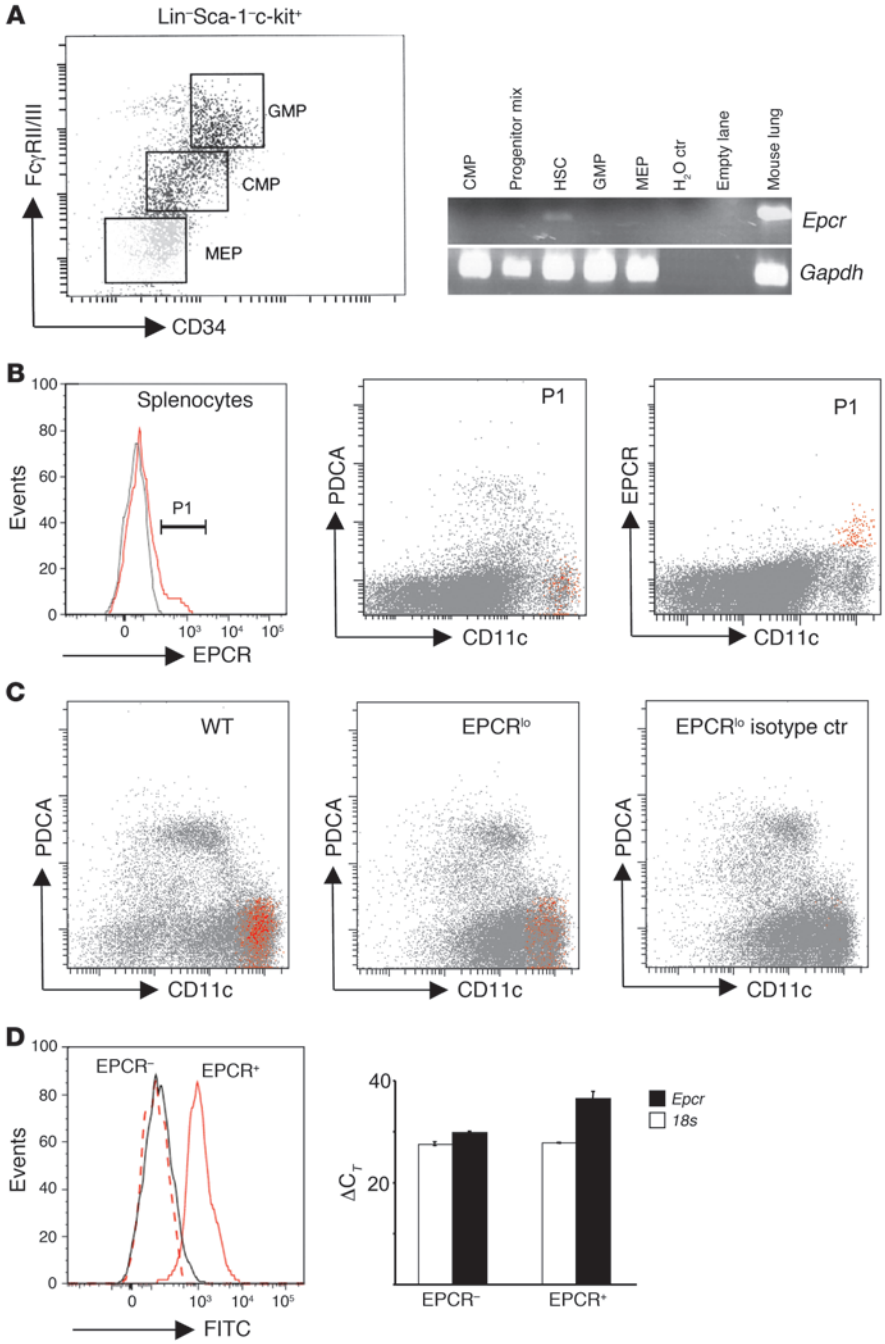

Figure 2
EPCR is expressed in HSCs and spleen DCs. (**A**) Whole BM from 10 wild-type mice was pooled and fractionated by FACS into HSCs (Lin⁻Sca-1^{hi}c-kit^{hi}; Lin: CD3ε, CD4, CD8a, CD19, Ly6G, CD45R), granulocyte-macrophage progenitors (GMP: Lin⁻Sca-1⁻c-kit⁺CD34⁺FcRγII/III^{hi}), common myeloid progenitors (CMP: Lin⁻Sca-1⁻c-kit⁺CD34⁺FcRγII/III^{lo}), megakaryocytic erythroid progenitors (MEP: Lin⁻Sca-1⁻c-kit⁺CD34⁻FcRγII/III^{lo}), or a progenitor mix (CMP, GMP, MEP, CLP: Lin⁻Sca-1⁻c-kit$^{lo/-}$). *Epcr* and *Gapdh* mRNA were amplified by 35- and 30-cycle RT-PCR, respectively, from RNA isolated from sorted cell pools. (**B**) Detection of EPCR expression in wild-type splenocytes. Back-gating of EPCR-positive cells (gate P1, gray line indicates signal obtained with isotype control antibody) shows EPCR expression in CD11c^{hi}PDCA-1⁻ DCs (red). (**C**) Abundance of EPCR-expressing CD11c^{hi}PDCA-1⁻ DCs is diminished in EPCR^{lo} mice. Spleen DCs were enriched by capture on CD11c/PDCA-1 magnetic beads and analyzed for EPCR expression as in **B**. (**D**) Detection of EPCR surface expression captures the majority of DCs expressing *Epcr* mRNA. Spleen DCs were enriched on magnetic beads as in **C**, and EPCR⁺ cells were isolated by FACS via gating on CD11c^{hi}PDCA-1⁻ DCs, followed by sorting into EPCR⁺ and EPCR⁻ CD11c^{hi}PDCA-1⁻ cells (left panel, solid gray line: isotype control on post-sort EPCR⁺ cells; dotted red line: FITC intensity of post-sort EPCR-depleted CD11c^{hi}PDCA-1⁻ cells; solid red line: FITC intensity of post-sort EPCR⁺ CD11c^{hi}PDCA-1⁻ cells). Quantitative RT-PCR analysis of *Epcr* mRNA on sorted cells shows depletion of *Epcr* mRNA in cells lacking EPCR surface expression as detected by flow cytometry (right panel; bars indicate the average ± SD of the detection threshold expressed as the ΔC_T value for *Epcr* mRNA determined in 2 independent sorting experiments, with 3 measurements/sample).

tance of EPCR and PAR1 expression in BM-derived cells for the efficacy of aPC therapy in the same experimental model of acute LPS-induced inflammation that was employed earlier to document the PAR1 and EPCR dependence of the mortality-reducing effect of 5A-aPC (4). To this end, mice with selective EPCR or PAR1 deficiency in immune cells and non-hematopoietic cells such as endothelium, respectively, were derived by reciprocal BM transfers between wild-type mice and animals expressing greatly diminished levels of EPCR (EPCR^{lo}) or devoid of PAR1 expression (PAR1-null). All BM chimeras exhibited normal reconstitution (≥90% at 8 weeks) of the hematopoietic system with donor-derived cells, and control experiments (wild-type marrow into CD45 isotype–mismatched wild-type recipients) showed that the BM transfer procedure per se did not alter endotoxemia survival or responsiveness to aPC (Figure 1A). Mice with EPCR deficiency restricted to immune cells exhibited the same baseline sensitivity to LPS challenge as control animals, as reflected in 7-day mortality; however, aPC infusion completely failed to reduce mortality in these animals (Figure 1B). Selective reduction of EPCR function on non-BM-derived cells (i.e., endothelium) likewise rendered the animals refractory to the mortality-reducing effect of aPC treatment (Figure 1C). Corresponding experiments with PAR1-deficient mice confirmed earlier observations that complete PAR1 deficiency does not alter survival of an LD_{50} LPS challenge (data not shown) and revealed that

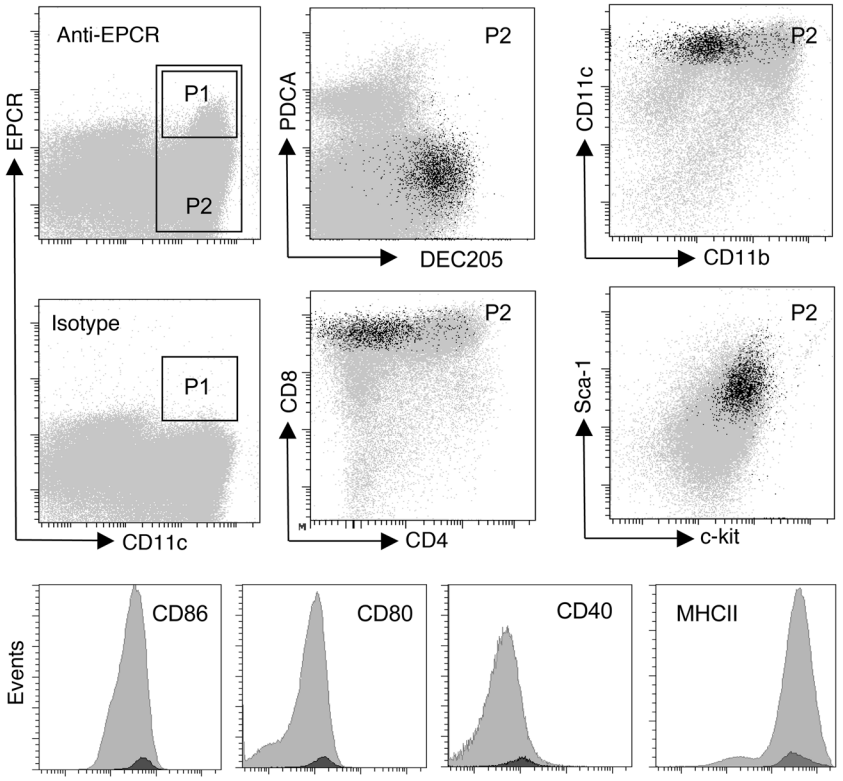

Figure 3
EPCR is expressed in the CD8$^+$DEC205$^+$ subset of spleen DCs. Spleen DCs were enriched by capture on CD11c/PDCA-1 magnetic beads, and EPCR$^+$ cells in gate P1 were back-gated onto the CD11^{hi} population defined by gate P2 (gray events) to visualize EPCR expression (black events) in relation to the indicated markers.

PAR1 expression on BM-derived cells was necessary for mortality reduction by aPC (Figure 1D). Of note, mice with selective PAR1 deficiency in non-hematopoietic cells exhibited the same mortality as wild-type animals in the absence of aPC treatment, but aPC improved overall mortality with borderline significance ($P = 0.09$; Figure 1E) and prolonged the time of survival in a statistically significant manner ($P = 0.0004$; Mantel-Cox log-rank analysis).

These results formally confirm that EPCR and PAR1 are necessary not only for the therapeutic efficacy of normal aPC, as shown earlier (4), but also for the efficacy of the signaling-selective 5A-aPC variant, and clearly document that responsiveness to therapy with exogenous 5A-aPC requires normal EPCR and PAR1 expression on BM-derived immune cells.

EPCR expression in hematopoietic progenitor cells and spleen DCs. To identify the candidate in vivo cellular targets of aPC among BM-derived cells, immune cell populations of normal wild-type mice were surveyed for expression of the aPC receptor EPCR. Confirming earlier findings (20, 21), expression of EPCR antigen, detected by staining and fluorescence-activated cell sorting (FACS) analysis with anti-EPCR antibody in lineage-negative (Lin$^-$) BM precursor cells, was detected in putative HSCs (Lin$^-$Sca-1^{hi}c-kit^{hi} side population [SP] cells; Hoechst 33342 efflux side population; data not shown). RT-PCR analysis of mRNA isolated from sorted progenitors confirmed that EPCR transcripts were only present in HSCs but not in granulocyte-macrophage progenitors (Lin$^-$Sca-1$^-$c-kit$^+$CD34$^+$FcRγII/III^{hi}), common myeloid progenitors (Lin$^-$Sca-1$^-$c-kit$^+$CD34$^+$FcRγII/III^{lo}), or megakaryocytic erythroid progenitors (Lin$^-$Sca-1$^-$c-kit$^+$CD34$^-$FcRγII/III^{lo}) (Figure 2A). In addition, as reported by others, EPCR was expressed in a not-further-defined population of Lin$^+$ marrow cells, which did not express CD11c (data not shown).

Among steady-state mature immune cells, surface expression of EPCR as detected by fluorescence-labeled EPCR-specific antibody was absent from circulating, spleen, or peritoneal monocytes (F4/80$^+$CD11b$^+$Mac3$^+$), neutrophils (Gr1$^+$CD11b^{lo}), B cells (B220$^+$CD19$^+$), T cells (NK1.1$^-$CD3ε$^+$CD4/CD8$^+$ subsets), NK cells (NK1.1$^+$CD3ε$^-$), NK T cells (NK1.1$^+$CD3ε$^+$), and other CD45$^+$CD11c$^-$ leukocytes. Positive staining was associated with a subset of PDCA-1$^-$CD11c^{hi} DCs that constitute between 5% and 10% of the total CD11c^{hi} DC population in the spleen (8.6 ± 5, average ± SD; $n = 7$; Figure 2B). In the spleen of EPCR^{lo} mice, the abundance of cells detected by FITC–anti-EPCR antibody was reduced 5-fold (1.7% ± 1% EPCR$^+$ among CD11c^{hi} cells) as compared with that in wild-type mice (Figure 2C).

No additional target cell populations for aPC were identified using FITC-labeled recombinant aPC, or biotinylated aPC in combination with streptavidin-FITC. In order to examine whether cell surface EPCR detection with fluorophore-labeled anti-EPCR antibody was sufficiently sensitive to identify all EPCR-expressing cells, splenocytes were selected on CD11c/PDCA-1 magnetic beads, followed by FACS sorting of the EPCR$^+$ and the EPCR$^-$ subpopulations of CD11c^{hi}PDCA-1$^-$ cells. Quantitative RT-PCR analysis of *Epcr* mRNA levels in the sorted populations showed that selection of EPCR$^+$ cells by flow cytometry resulted in approximately 12-fold enrichment of *Epcr* mRNA, indicating that cell surface EPCR antigen detection by the employed protocol captured at least 90% of the cell population expressing *Epcr* mRNA (Figure 2D).

Characterization of EPCR-expressing DCs. To characterize the steady-state EPCR$^+$ DC subset in the spleen, splenocytes expressing CD11c or PDCA-1 were selected on CD11c/PDCA-1 magnetic beads, followed by flow cytometric sorting of EPCR$^+$ cells expressing high levels of CD11c (gate P1 in Figure 3) or a PDCA-1$^{lo/-}$CD11c^{hi}

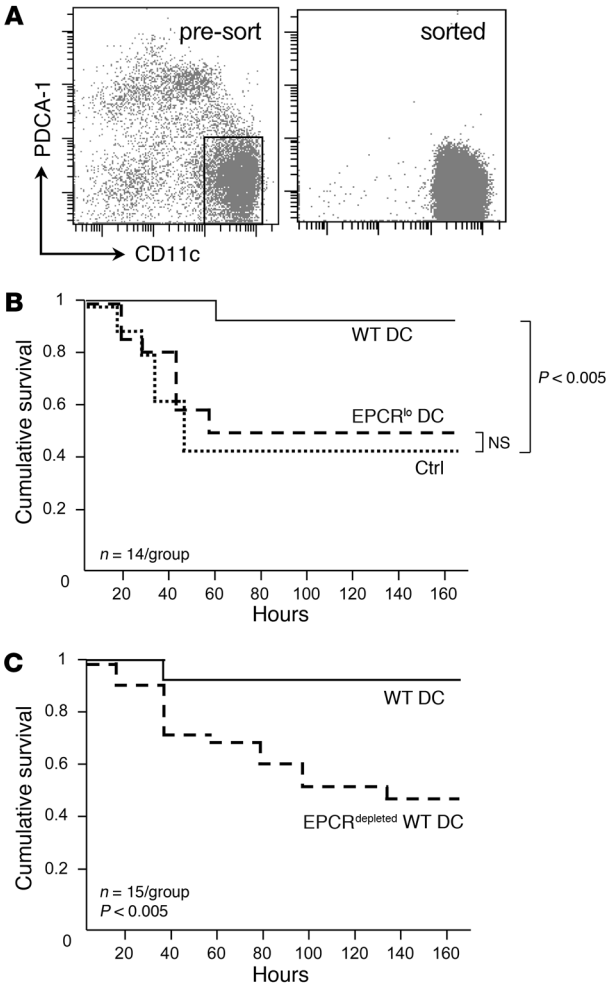

Figure 4
EPCR$^+$ DCs are required for the therapeutic efficacy of 5A-aPC. (**A**) Spleen DCs were enriched by selection on CD11c/PDCA-1 magnetic beads from unchallenged wild-type or EPCR^{lo} mice, and the CD11c^{hi}PDCA-1$^-$ population was isolated by preparative FACS. (**B**) Sorted DCs (10^6) were infused intravenously into mice with hematopoietic EPCR deficiency, treated 24 hours later with LPS/5A-aPC, and monitored for 7-day survival. A control group (ctrl) received wild-type DCs and LPS/S360A-aPC. (**C**) In an independent experiment, mice with hematopoietic EPCR deficiency received either wild-type DCs or wild-type DCs depleted of EPCR$^+$ cells, followed by treatment with LPS/5A-aPC. Efficacy of 5A-aPC was measured by Kaplan-Meier log-rank analysis of survival.

population comprising both EPCR$^+$ and EPCR$^-$ cells (gate P2 in Figure 3). Global gene expression analysis on Affymetrix Mouse Genome 430 version 2 Arrays detected 145 uniquely annotated transcripts that exhibited an at least 4-fold increase in abundance in the EPCR$^+$ population relative to the CD11c$^+$PDCA-1$^{lo/-}$ population (Supplemental Excel file 1; supplemental material available online with this article; doi:10.1172/JCI42629DS1). These regulated transcripts included the DC marker Ly-75/DEC205, the chemokine Cxcl9/MIG, the regulator of proteasome function Zfand2a/AIRAP, the histone demethylase jmjd3, the transcription factors atf3 and Nr4a2/Nurr1, and the prostaglandin E2 biosynthesis enzyme cyclooxygenase-2 (cox-2/ptgs2). This exploratory analysis indicated that EPCR expression was potentially associated with the DEC205$^+$CD8$^+$ DC subset in the spleen. As judged from quantitative RT-PCR analysis, *DEC205* mRNA was indeed enriched approximately 12-fold in EPCR-selected CD11c$^+$ DCs. Analysis by flow cytometry confirmed that EPCR$^+$ spleen CD11c^{hi} DCs exhibited a CD4$^-$CD8$^+$CD205$^+$CD11b^{lo}MHC class II$^+$ phenotype and, compared with the total CD11c^{hi} population, relatively high surface expression of the DC markers CD40, CD80, and CD86. In addition, EPCR$^+$ cells expressed high levels of the lineage markers *Sca-1* and *c-Kit* (Figure 3). Within the limits of detection, at most 10% of EPCR$^+$ cells lack surface expression of CD8a or CD205. Conversely, only approximately 30% (30 ± 10, average ± SD; $n = 4$) of CD8$^+$CD205$^+$CD11c^{hi} DCs expressed EPCR at levels above the threshold of detection. The overall abundance of CD11c^{hi} DCs and the abundance of the CD8$^+$CD11c^{hi} subpopulation (~22% of spleen DCs) were identical in wild-type and EPCR^{lo} mice.

EPCR$^+$ spleen DCs are necessary for responsiveness to aPC therapy. In order to directly test the in vivo importance of EPCR-expressing DCs, and to distinguish the role of EPCR-expressing BM precursors from that of EPCR$^+$ DCs as the relevant targets of aPC, we measured the ability of spleen-resident cell populations to restore responsiveness to aPC therapy in mice with reduced hematopoietic EPCR expression (which are completely refractory to aPC treatment, as shown above). To this end, DCs were enriched by selection of splenocytes from unchallenged wild-type and EPCR^{lo} mice on magnetic anti-CD11c and anti–PDCA-1 beads, followed by FACS of CD11c^{hi}PDCA-1$^-$ cells (Figure 4A). The sorted populations contained less than 1% of contaminating granulocytes, B, T, or NK/NK T cells, and less than 5% of CD11b$^+$F4/80$^+$ monocytes (Supplemental Figure 1) and constituted approximately 50% viable cells, as judged by DAPI staining. DCs (1×10^6) sorted from the spleen of wild-type or EPCR^{lo} mice were then intravenously injected into BM chimeras with normal levels of EPCR in non-hematopoietic tissues but diminished receptor expression in DCs (generated by transfer of EPCR-deficient BM into lethally irradiated wild-type recipients; see above). Twenty-four hours later, the animals were challenged with LPS and given a bolus infusion of 10 μg 5A-aPC or proteolytically inactive S360A-aPC (control). Transfer of EPCR-sufficient wild-type CD11c^{hi} DCs into BM chimeras with low EPCR expression in hematopoietic cells restored the ability of 5A-aPC to reduce mortality to a similar extent as in EPCR-sufficient wild-type mice (Figure 4B). Conversely, adoptive transfer of CD11c^{hi} DCs isolated from EPCR^{lo} mice did not restore the efficacy of aPC treatment (Figure 4B). Likewise, adoptive transfer of wild-type CD11c^{hi} DCs depleted of EPCR$^+$ cells by fluorescence-activated sorting did not improve survival of aPC-treated mice with hematopoietic EPCR deficiency (Figure 4C). These outcomes show that CD11c^{hi} DCs expressing normal levels of EPCR, i.e. the EPCR$^+$CD205$^+$CD8$^+$CD11c^{hi} DC subset, are a physiologically relevant BM-derived cellular target of 5A-aPC that is required for the survival-enhancing effect of aPC therapy in a mouse model of lethal endotoxin challenge.

5A-aPC suppresses the in vivo LPS response of EPCR$^+$ DCs. To characterize how 5A-aPC infusion altered the response of EPCR$^+$ DCs to LPS, this DC subset was isolated by magnetic bead immunoselection and preparative FACS of splenocytes as described above and subjected to a global gene expression analysis. Testing of 2 independent EPCR$^+$ DC samples (each pooled from 6 mice) at

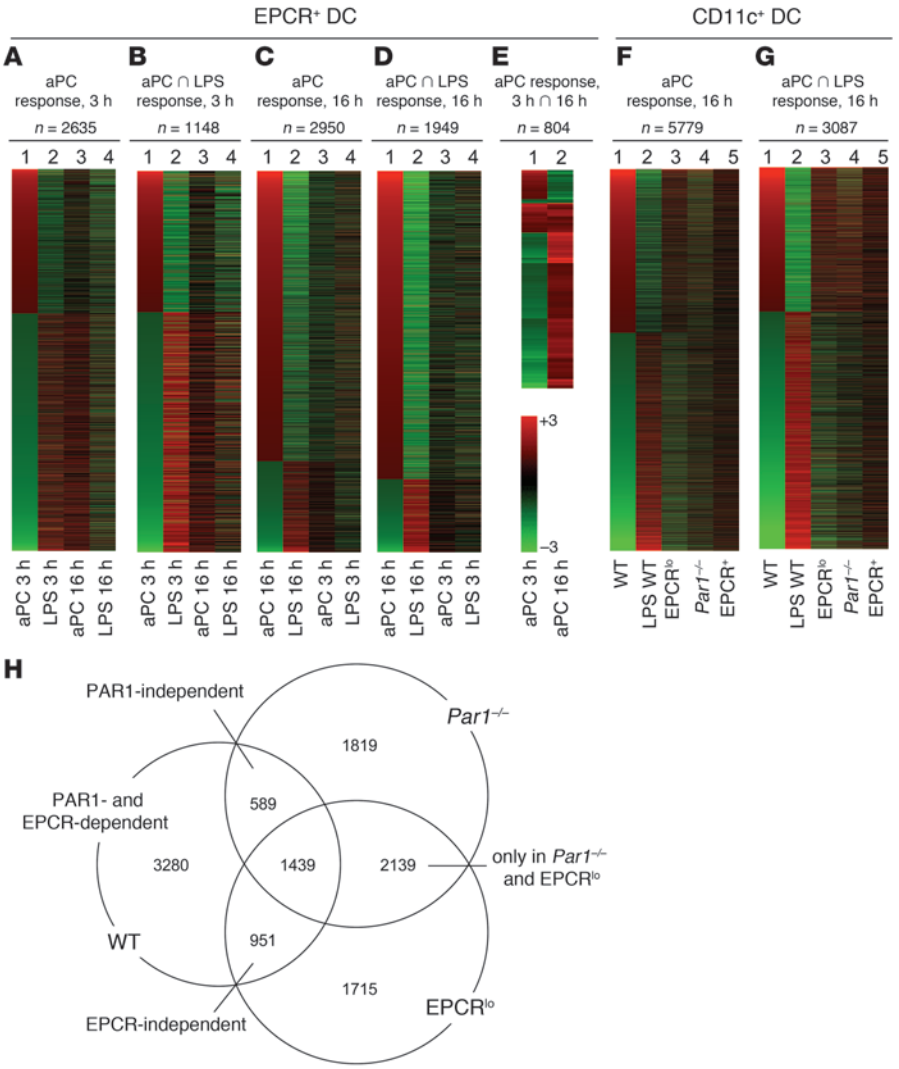

Figure 5

APC effects on LPS-induced gene expression in DCs. (**A**–**G**) Heat maps depicting the effect of aPC treatment on the mRNA abundance of specific sets of genes, analyzed in FACS-selected EPCR$^+$ DCs (**A**–**E**) or in sorted CD11c^{hi} spleen DCs comprising the EPCR$^+$ and EPCR$^-$ populations (**F** and **G**). The number of probe sets represented in each heat map is indicated. (**A**) Lane 1: Genes exhibiting a more than 2-fold up-/downregulation (average of 2 independent experiments) in EPCR$^+$ cells isolated 3 hours after LPS challenge/5A-aPC administration, as compared with the equivalent sample isolated from mice receiving LPS and the proteolytically inactive S360A-aPC variant. Lanes 2 and 4: Behavior of the same set of genes in cell samples isolated 3 or 16 hours, respectively, after exposure of mice to LPS/S360A-aPC, as compared with EPCR$^+$ cells isolated from the spleen of unchallenged mice. Lane 3: aPC response of the same set of genes 16 hours after exposure to LPS/5A-aPC, as compared with LPS/S360A-aPC. (**B**) Subset of the genes in **A** regulated ≥2-fold in mice treated with LPS/S360A-aPC. (**C**) Lane 1: Set of probes with ≥2-fold up-/downregulation in EPCR$^+$ cells isolated 16 hours after LPS challenge/5A-aPC administration, as compared with the equivalent sample isolated from mice receiving LPS/S360A-aPC. The set of genes in this map is largely non-overlapping with the gene set depicted in **A** and **B**. (**D**) Subset of the genes analyzed in **C** that also responds to LPS/S360A-aPC. (**E**) Subset of genes shown in **A** and **C** that respond to 5A-aPC treatment (≥2-fold up-/downregulated) at both time points. (**F**) Lane 1: Differential mRNA abundance of genes detected in CD11c$^+$ cells isolated from LPS-challenged wild-type mice as 5A-aPC responsive (≥2-fold different, compared with treatment with S360A-aPC). Lane 2: Response of this gene set to LPS/S360A-aPC treatment, as compared with mice that were not challenged with LPS. Lanes 3 and 4: aPC response of these genes (relative change in abundance in mice receiving LPS/5A-aPC, as compared with mice receiving LPS/S360A-aPC) in CD11c^{hi} DCs in isolated from *Par1*$^{-/-}$ and EPCR^{lo} mice. Lane 5: aPC response of this gene set in EPCR$^+$ DCs isolated from wild-type mice. (**G**) Behavior of the 5A-aPC–responsive subset of the genes in **F** that is also regulated in mice receiving LPS/S360A-aPC. (**H**) Relation of 5A-aPC–responsive genes (≥2-fold up- or downregulated at 16 hours in LPS/5A-aPC–treated mice, as compared with LPS/S360A-aPC–treated animals) identified in CD11c$^+$ cells isolated from wild-type, *Par1*$^{-/-}$, and EPCR^{lo} mice. Numbers denote regulated probe sets unique to or shared in animals with a given genotype. Data are based on the array hybridization intensity of a normalized pool of 6 independent samples for each genotype; control RT-PCR experiments verified that the abundance of select mRNAs in the pooled samples as detected by array hybridization accurately reflected mRNA abundance in each of the individual samples used to generate the pool.

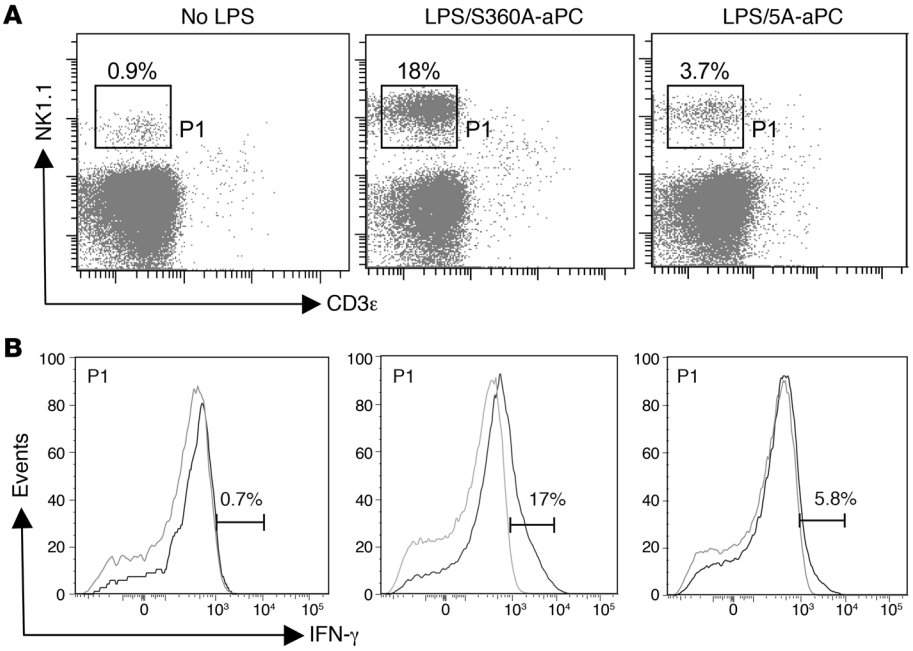

Figure 6
APC alters the function of IFN-producing NK-DCs. Spleen DCs were isolated from unchallenged (no LPS), LPS/S360A-aPC–treated, and LPS/5A-aPC–treated mice (14–16 hours after LPS challenge) by selection on CD11c/PDCA-1 magnetic beads, followed by FACS gating on cells expressing high levels of CD11c, as in Figure 4A. (**A**) Expression of the surface markers NK1.1 and CD3ε live cells. (**B**) Detection of intracellular IFN-γ in permeabilized $CD11c^+PDCA\text{-}1^-CD3\varepsilon^-NK1.1^+$ cells (gray line indicates isotype control staining for IFN-γ). Data shown are derived from one individual mouse each and are representative of 3 independent experiments.

3 hours and 16 hours after LPS exposure showed that 5A-aPC treatment was associated with substantial changes in gene expression at the 3- and 16-hour time points (3 hours: 60 upregulated/149 downregulated ≥4-fold, 913 upregulated/1,722 downregulated ≥2-fold; 16 hours: 280 upregulated/30 downregulated ≥4-fold, 2,181 upregulated/769 downregulated ≥2-fold; Supplemental Excel file 1). The behavior of these aPC-regulated transcripts is shown in Figure 5A (3-hour time point) and Figure 5C (16-hour time point). The opposing directionality in gene expression (Figure 1A, compare lanes 1 and 2) at the 3-hour time point indicates that aPC treatment in essence silences a specific subset of the transcriptional response to LPS challenge in the analyzed cell populations. This early effect of 5A-aPC is, albeit still recognizable in the set of transcripts that are increased by aPC treatment at the 3-hour time point, substantially diminished at the 16-hour time point (Figure 5A, compare lane 3 with lane 2). The entire set of the 3-hour aPC response genes was underrepresented ("downregulated") 16 hours after LPS challenge and therefore likely represents an aspect of the LPS response that is triggered early but subsides toward the 16-hour time point. Figure 5B depicts the subset of the aPC-responsive genes shown in Figure 5A that are not only regulated by aPC, but also respond to LPS exposure per se. This inflammatory subset of the 3-hour aPC response comprises 49 of 209 probe sets (23%) regulated at least 4-fold and 1,148 of 2,728 (42%) regulated at least 2-fold. The overall heat map patterning resembles that of the total aPC response shown in Figure 5A but becomes more pronounced. The smaller intensity differential in Figure 5B, lane 4 as compared with lane 2, again suggests that the 3-hour 5A-aPC response affects a subset of the LPS response that is more pronounced in the early phase of endotoxemia.

Figure 5, C and D, represents a corresponding analysis of the entire 16-hour aPC response (Figure 5C) and the "inflammatory subset" thereof (Figure 5D: 203 of 310, 65% regulated ≥4-fold; 1,949 of 3,057, 64% regulated ≥2-fold). It is noteworthy that the sets of aPC-responsive genes at the 3- and 16-hour time points were largely non-overlapping (only 197 shared probe sets). Although the set of genes analyzed in Figure 5, C and D, is therefore nearly completely distinct from the transcripts identified in Figure 5, A and B, the overall pattern is similar with respect to the fact that aPC again suppresses a specific (albeit different) subset of the late LPS response. Only a small fraction of genes responded to aPC in a concordant manner at both the 3-hour and 16-hour time points (n = 75 with ≥2-fold higher or lower abundance at 3 and 16 hours; Figure 5E, lanes 1 and 2; Supplemental File 2), whereas the remainder of the genes responding to aPC at both time points showed opposing effects of 5A-aPC at 3 hours and 16 hours. While less pronounced, this trend can also be noted in Figure 5, A–D (note complementary shading in lane 1 versus lane 3).

Previous analyses (4) had shown that 5A-aPC treatment did not significantly alter systemic cytokine abundance in plasma of LPS-challenged wild-type mice. Cytokine levels in total spleen homogenates prepared 16 hours after LPS exposure likewise failed to correlate cytokine abundance with 5A-aPC treatment (Supplemental Table 1). A corresponding analysis of splenocytes at the 3-hour time point indicated modest, reproducible alterations associated with aPC treatment, the most pronounced effects (≥2-fold increase) being noted for IL-10, eotaxin, GM-CSF, and RANTES (Supplemental Table 2). Intracellular levels of IL-12p40 in sorted $EPCR^+$ DCs, measured 16 hours after LPS exposure by fluorescence cytometry, were not altered by aPC treatment (data not shown). The above analyses of gene expression patterns in $EPCR^+$ cells likewise failed to detect significant changes in the mRNA levels of these mediators (Supplemental Tables 1 and 2) and are consistent with the absence of a pronounced systemic antiinflammatory effect of aPC on the cytokine/chemokine profile measured in plasma or whole spleen lysates.

aPC exerts EPCR- and PAR1-independent antiinflammatory effects on DCs. To determine whether the effect of 5A-aPC on the mRNA expression changes in response to LPS were limited to $EPCR^+$ DCs, we conducted a corresponding gene expression analysis on the entire $CD11c^{hi}$ pool of spleen DCs, sorted from a PDCA-1 versus CD11c scatter plot of splenocytes selected on PDCA-1/CD11c

magnetic beads, as indicated in Figure 4A. 5A-aPC treatment was associated with a markedly altered expression profile as measured 16 hours after LPS challenge (2,703 upregulated, 3,076 downregulated; ≥2-fold; Figure 5F, lane 1). This gene set overlapped only to a minor extent with the 16-hour or 3-hour 5A-aPC–responsive gene set identified in sorted EPCR$^+$ cells shown in Figure 5, A–E (compare lanes 1 and 5 in Figure 5F). Akin to the result seen with EPCR$^+$ DCs, aPC administration counteracted a distinct subset of the LPS response (Figure 5F, lane 2), i.e., eliciting an effect opposite that of LPS on the abundance of these transcripts. This pattern was still recognizable, although in a less pronounced manner, in equivalent cell samples isolated from LPS/5A-aPC–treated EPCR^{lo} mice (Figure 5F, lane 3), but was essentially abolished in samples isolated from LPS/5A-aPC–treated *Par1*$^{-/-}$ mice (Figure 5F, lane 4). The inhibitory effect of 5A-aPC on the LPS response of CD11c^{hi} cells was again more pronounced in the subset of aPC-responsive genes that were also regulated in mice receiving LPS together with inactive aPC variant S360A-aPC ("inflammatory subset"). In contrast to the overall 5A-aPC response shown in Figure 5F, the effect of 5A-aPC on the LPS-responsive, inflammatory gene subset was partially preserved not only in EPCR^{lo} mice, but also in *Par1*$^{-/-}$ mice (compare Figure 5F, lane 4, and Figure 5G, lane 4).

This complexity of DC responses to aPC is illustrated by the Venn diagram shown in Figure 5H: applying a threshold of at least 2-fold up- or downregulation, we detected 3,280 of 5,779 probe sets as aPC responsive in wild-type mice, but not in PAR1-null mice or EPCR^{lo} mice. This set therefore represents an aPC response in wild-type animals that is dependent on normal expression of both receptors. It is further evident that aPC elicited robust responses in EPCR^{lo} as well as in PAR1-null mice that were not seen in wild-type animals. The aPC effects on approximately 50% of genes in this set required neither PAR1 nor EPCR (Figure 5H: intersection of the aPC response in *Par1*$^{-/-}$ and EPCR^{lo} mice not shared with the response in wild-type mice; n = 2,139). Such EPCR- and PAR1-independent aPC responses therefore represent experimental artifacts that are only revealed in the absence of these receptors.

5A-aPC inhibits IFN-γ production by CD11c$^+$NK1.1$^+$cells. In response to inflammation, CD11c expression may potentially be acquired by additional cell types not present in the spleen of unchallenged mice, including monocyte-derived DCs and TNF-α– and iNOS-producing DCs (TIP-DCs) (23), as well as IFN-producing cells expressing the NK cell marker NK1.1 and cytolytic NK cell products such as perforin and granzyme B (24–28). The expression profile elicited by aPC treatment in CD11c$^+$ DCs was indeed notable for the fact that a number of the most significantly diminished transcripts encoded gene products characteristically associated with NK cells, including NK cell receptors and IFN-γ (Supplemental Excel file 1). This aPC-mediated reduction in *Ifng* mRNA abundance persisted in EPCR-deficient, and to a somewhat lesser extent also in PAR1-deficient, mice, yet was not observed in wild-type mice treated with the proteolytically inactive S360A-aPC variant (Supplemental Excel file 1), suggesting that this aPC effect is dependent on the proteolytic activity of 5A-aPC but may not require normal expression levels of EPCR or PAR1. Flow cytometric analysis of splenocytes confirmed that LPS exposure induced the appearance of a distinct PDCA-1$^-$CD11c$^+$ cell population that produced IFN-γ (Figure 6) and expressed the NK cell marker NK1.1, CD11c, B220, but not EPCR (Supplemental Figure 2). In accordance with the above expression profiling data, aPC treatment reduced between 2- and 3-fold the absolute number of CD11c$^+$B220^{int}NK1.1$^+$CD3ε$^-$ cells (LPS/S360A-aPC: 11.7% ± 5% of CD11c$^+$; LPS/5A-aPC: 4.7% ± 1.6%; no LPS: 2% ± 1%), as well as by approximately 4-fold the extent of IFN-γ production by these cells present in the spleen of LPS-challenged mice (Figure 6B). The abundance of the unrelated inflammatory subset of TIP-DCs and the extent of iNOS production (revealed by detection of intracellular iNOS) by these cells were not altered by aPC treatment (data not shown). Analysis of lymph nodes (isolated 14–16 hours after LPS challenge; mesenteric, mediastinal, inguinal) by histology and immunohistology with HRP-conjugated antibodies against Nimp-14, CD45, CD11c, and Mac3 and by flow cytometry to detect Gr-1 (ly6-C/ly6-G), CD11c, CD11b/Mac-1, and Mac-3 did not show any significant aPC-mediated effects on overall size/cellularity or DC content (data not shown).

Discussion

The purpose of the present study was to gain insight into how the effector protease of the protein C anticoagulant pathway, aPC, alters the host immune response to inflammatory challenges. Previous studies provided evidence that the ability of therapeutically administered aPC to reduce mortality of LPS-induced endotoxemia and of bacterial sepsis required normal expression of the aPC receptor EPCR and PAR1 (3, 4). Based on this information, we therefore sought to identify the critical EPCR-expressing cellular targets on which aPC acts to reduce mortality in mouse models of lethal inflammation. The initial series of experiments employed straightforward BM transfer experiments to delineate the relative importance of EPCR and PAR1 expression on hematopoietic cells, as compared with non-BM-derived cell types. These experiments unequivocally revealed that mortality reduction by aPC required normal expression of both receptors on radiation-sensitive hematopoietic cells. An unexpected finding was that selective PAR1 expression in hematopoietic cells was sufficient for sustaining partial aPC responsiveness (trend toward 7-day mortality reduction; significant prolongation of survival time). This suggests that the protective effect of aPC infusion against the inflammation-induced breakdown of the vascular permeability barrier, which is thought to be based on PAR1 engagement via the aPC-EPCR complex on the surface of endothelial cells, either does not contribute significantly to mortality reduction by aPC in the experimental setting employed here or is not strictly dependent on endothelial PAR1 expression. On the other hand, loss of PAR1 function from radiation-sensitive hematopoietic cells abolished the response to treatment with the signaling-selective 5A-aPC variant, dovetailing with the requirement for hematopoietic expression of EPCR. These observations strongly indicated that aPC must interact with EPCR and PAR1 on BM-derived immune cells to suppress lethal inflammation.

To identify the relevant cellular target of aPC, we analyzed the expression pattern of EPCR on hematopoietic cells. In contrast to the reported fairly wide distribution of this receptor on human innate immune cells, we identify a subset of CD8$^+$CD11c^{hi} DCs as the only murine immune cell population other than hematopoietic precursors that expresses readily detectable levels of EPCR on their cell surface. Since adoptive transfer of EPCR$^+$ DCs, but not of EPCR-deficient DCs or normal DCs depleted of EPCR-expressing cells isolated from the spleen of non-challenged mice, restored responsiveness to aPC therapy, we conclude that the EPCR$^+$ DC subpopulation is a necessary target for the EPCR-dependent mortality-reducing activity of aPC.

CD8$^+$ DCs represent a distinct DC subpopulation whose emergence from the BM is controlled by the transcriptional regulator *Batf3/p21snft* (29). Compared with other DC populations, CD8$^+$ DCs exhibit a short in vivo half-life of approximately 1.5 days and are constitutively replenished from progenitors in the BM (30–33). The distinctly high expression of *Sca-1* and *c-Kit* in EPCR$^+$ DCs under baseline conditions might thus be related to their high turnover rate and indicate a more nascent or immature state. Specific functions associated with this DC population include the cross-representation of pathogen-derived antigens in the context of the class I MHC (reviewed in refs. 34–36); induction of CD8$^+$ T cell responses to viral pathogens, triggering a predominant T helper 1 type of response (37–40); highly efficient clearing of dying/apoptotic cells (41, 42); modulation of peripheral tolerance by inducing FoxP3$^+$ regulatory T cells (43) and tumor surveillance by cytotoxic T cells (29); and suppression of T cell–driven excessive inflammation secondary to induction of the tryptophan-metabolizing enzyme indolamine-2,3-deoxygenase (44). These recognized functions of CD8$^+$ DCs in the coordination of the adaptive immune responses provide a potential rationale for the surprisingly wide spectrum of inflammatory disease models, including the strictly T cell–driven neurodegeneration model of experimental autoimmune encephalomyelitis, in which aPC infusion has been shown to be beneficial (45). On the other hand, little is known about the specific function of these cells in immunity toward bacterial pathogens or in the host response to endotoxin. Existing data suggest that CD8$^+$ DCs are critical for efficient priming of T cell–dependent immunity toward viral and intracellular bacterial pathogens (reviewed in ref. 34). Adoptive transfer of CD8$^+$ spleen DCs ameliorates the pathology of infection with mycobacteria, likely by eliciting a more vigorous host response to limit bacterial growth and reducing the ensuing tissue damage (46), indicating that this particular DC subset is indeed a potent amplifier of the inflammatory host response. Attempts to correlate the effects of aPC on the LPS response of DCs with alterations in the chemokine/cytokine milieu in the plasma compartment and whole spleen lysates or via direct detection of intracellular IL-12 as a key modulator of DC function were not informative. Recent reports on the antiinflammatory effects of IL-10 in liver injury (47, 48) and in the suppression of graft-versus-host disease by CD8$^+$ DCs suggest that the statistically significant augmentation of IL-10 levels may be biologically relevant and possibly result from the interaction of EPCR$^+$ DCs with T cells (49). How aPC treatment affects the above candidate mechanisms and how they might contribute to mitigating the lethal effects of LPS challenge remains to be clarified.

Examination of the effect of aPC treatment on the global gene expression profile of EPCR$^+$ cells, or the subset of this response that required normal expression of both EPCR and PAR1, clearly showed that aPC treatment altered in a profound manner the overall expression profile of EPCR$^+$ DCs and completely inhibited a specific subset of the LPS response, thereby producing the striking complementary patterning of the heat maps shown in Figure 5, consistent with the notion that aPC treatment inhibits a marked antiinflammatory effect on the function of CD8$^+$ DCs. A limitation for the interpretation of the above gene expression analyses is that this approach cannot distinguish between direct effects on the transcriptional program of static, preexisting cell populations and an altered expression profile secondary to an altered cellular composition of the analyzed DC population under conditions of inflammation (33, 50–52). The reduced abundance and IFN-γ production of CD11c$^+$NK1.1$^+$ cells is one such example for aPC-induced population changes we were able to extract from the expression profile of CD11c^{hi} DCs. Flow cytometric characterization of various surface markers indicates that these cells are likely identical to the previously described population of so-called IFN-producing killer DCs (IK-DCs), which are frequently copurified with conventional DCs from mouse spleen and are a dominant source of IFN-γ among mouse DC subsets (25–28). In the context of infection, the cytotoxic activity of these cells is thought to provide initial protection against pathogens (26) and supports the DC-initiated clustering and activation of innate immune cells around infectious foci of *Listeria monocytogenes* (53). Although IK-DCs are necessary for the IFN-γ–dependent generation of TIP-DCs in the latter infection model, the abundance and iNOS elaboration of Tip-DCs in the spleen was not affected by aPC treatment in the LPS model employed in our study. IK-DCs have been proposed as the murine counterpart to human CD56$^+$ NK cells (25), which have been reported to express EPCR even in the absence of inflammation (19). However, we were unable to detect EPCR expression on the surface of mouse IK-DCs isolated from unchallenged or LPS-exposed mice or in other NK1.1$^+$ populations, and the suppression of IFN-γ production by aPC was not strictly dependent on EPCR. These observations indicate that this aPC effect is not sufficient for the EPCR-dependent mortality reduction by aPC and is not secondary to aPC effects on EPCR-expressing CD8$^+$ DCs. Importantly, this provides strong circumstantial evidence that the bioactivity of the signaling-selective 5A-aPC variant may not be limited to activation of EPCR- and/or PAR1-dependent signaling processes. Expression profiling of EPCR$^+$ DCs and the entire CD11c^{hi} DC population indeed revealed a remarkably complex effect of aPC treatment that was neither limited to EPCR$^+$ DCs nor strictly dependent on normal expression levels of PAR1 and EPCR and exhibited a markedly biphasic pattern. Such findings are entirely consistent with the notion that aPC not only engages the EPCR/PAR1 axis but interacts in addition with other signaling-competent receptors, including apoE receptor–2 (apoER2/lrp8), glycoprotein 1bα (GP1bα) (54, 55), CD11b/Mac-1 (F.J. Castellino, unpublished observation), and possibly as-yet-unknown aPC-selective receptors on monocytes (56). Integration of the dataset provided in Supplemental Excel file 1 with data from corresponding expression studies on mice lacking the various candidate receptors for aPC in specific cell types should eventually enable a systematic dissection of the specific intra- and intercellular pathways regulated by aPC over the time course of endotoxemia and infection.

Taken together, the results of this study represent to the best of our knowledge the first direct experimental evidence that the mortality-reducing effect of therapeutically administered, signaling-selective aPC variants requires engagement of EPCR on at least two different cellular targets, i.e., EPCR$^+$ DCs and non-hematopoietic cells (likely endothelium). The identification of spleen-resident, EPCR-expressing CD8$^+$DEC205$^+$ DCs as a relevant BM-derived cellular target establishes a previously unknown link between the protein C pathway and innate immunity. Given the established regulatory role of DCs in innate and adaptive immune responses, identification of this immune cell population as a functional target of aPC provides a strong incentive to examine the function of recombinant as well as endogenous aPC in settings other than endotoxemia, such as viral infections, T cell responses to antigen exposure, maintenance of peripheral self tolerance, and graft-versus-host disease. The in vivo gene expression analyses strongly

suggest that aPC's cell signaling effects on DC function to a substantial extent involve receptors/mechanisms other than signaling through EPCR and PAR1. For example, EPCR$^+$ DCs isolated 16 hours after exposure to LPS also express sphingosine kinase 1 (*Sphk1*) and the sphingosine-1-phosphate receptor $S1P_3$, as well as the frizzled 5 receptor (*Fzd5*) (Supplemental Excel file 1). These receptors are known to control the migration of DCs through the lymphatic system selectively in severe, late-stage endotoxemia (57) and to regulate aPC-sensitive, proinflammatory Wnt5a-Frz5 interaction signaling pathways (17). In aggregate, such observations suggest that various DC subsets are the critical innate immune cell population on which pro- and antiinflammatory effects of the coagulation system proteases aPC and thrombin are integrated.

An important question to be resolved is to what extent insights into mechanisms underpinning the efficacy of aPC therapy in mouse models can be exploited to improve the clinical practice of sepsis therapy. Species-specific differences in innate immune cell populations between mice and humans make it difficult to correlate EPCR-expressing CD8$^+$ DCs in the mouse spleen with specific human DC subsets (58, 59). Human blood-derived DCs expressing the cofactor for the thrombin-dependent formation of aPC, thrombomodulin/Thbd (BDCA-3/CD141) have been proposed as the functional equivalent of murine CD8$^+$DEC205$^+$ DCs (60–62). Analysis of blood samples collected from 3 different healthy donors failed to produce evidence for EPCR expression in this circulating DC type (our unpublished observations), and it remains to be investigated whether EPCR expression in spleen-resident DCs is conserved between humans and mice.

Current knowledge about the cellular and molecular targets mediating aPC's various bioactivities indicate that its therapeutic effect in the setting of sepsis may be highly context dependent and vary over the time course of acute inflammatory challenges. For example, the clearly documented beneficial effects of aPC in the limited subsets of patients with progressed, severe sepsis may largely be based on its proteolytic activity toward proinflammatory histones released from damaged organs (2) and the suppression of thrombin generation, which may mitigate progressive systemic coagulation activation and potentially inhibit the dissemination of inflammatory innate immune cells through the lymphatic system (57). Given that DCs, including the EPCR$^+$ subset identified here, likely are essential for mounting an efficient host response to pathogens in the early stages of infection, we suspect that suppression of the proinflammatory function of these cells in the early stages of sepsis may only be beneficial as long as pathogen load can be controlled through supporting measures, such as treatment with antibiotics. On the other hand, preliminary studies also provided evidence that aPC treatment in the early stage of LPS challenge was associated with increased abundance of EPCR-expressing hematopoietic precursors and expansion of immature myeloid populations in the BM in the late stages of endotoxemia (our unpublished observations). While the outcomes of adoptive cell transfer experiments clearly document that such effects of aPC on hematopoietic precursors are not necessary for responsiveness to aPC infusion at the very onset of acute endotoxemia, they may become highly relevant in different experimental models of infection (for example, by ameliorating the apoptotic loss of DCs and thereby the extent of secondary "immune paralysis" as a consequence of sepsis; refs. 63, 64). The identification of DCs as a novel, biologically relevant target of aPC therapy in the mouse substantiates the concept that aPC not only modulates a remarkably wide spectrum of host responses to inflammation and infection, but does so through multiple pathways involving interaction with distinct substrates/receptors on a variety of cellular targets. Although the precise cellular and molecular targets of aPC may vary between species, this general concept is likely transferable to human biology, and defining aPC's effects on specific subsets of the host response to inflammatory injury may hold the key for understanding the current limitations of clinical aPC therapy.

Methods

Animals. C57BL/6 and B6.SJL [B6-Ptprc(d)Pep3(b)/BoyJ] mice were obtained from Charles River Laboratories and The Jackson Laboratory, respectively. EPCR^{lo} and PAR1-knockout mice have been described previously (65–67). All experiments in the current study were performed on sex- and age-matched animals exhibiting an C57BL/6 genetic background (≥10 backcrosses). Experiments involving animals adhered to the NIH *Guide for the care and use of laboratory animals* (publication no. 85-23. Revised 1985) and were approved by the Medical College of Wisconsin's Institutional Animal Care and Use Committee.

Chemicals and reagents. Recombinant murine active site mutant aPC (S360A-aPC) and mutant aPC (5A-aPC) were characterized and produced as described previously (4, 68). LPS (*E. coli* O55:B5) and collagenase were purchased from Sigma-Aldrich. Cytokine assays were performed using the 23-Plex Group 1 Pro Mouse Cytokine Assay (Bio-Rad).

Isolation of DCs from spleen. Spleen tissue was minced and incubated in collagenase solution (2 mg/ml in 10 mM HEPES, 150 mM NaCl, 5 mM KCl, and 1 mM $MgCl_2$) for 30 minutes at 37°C. Single cell suspensions were prepared by passing through a 70-μM filter; red blood cells were lysed in 150 mM NH_4Cl; and splenocytes were suspended in phosphate-buffered saline (pH 7.2), 0.5% BSA, and 2 mM EDTA, treated with Fc-blocking CD16/CD32 antibody (0.5 μg/1 × 10^6 cells). Enrichment of DCs was performed by two rounds of positive selection on mouse PanDC magnetic microbeads (Miltenyi Biotec) according to the supplier's instructions.

Flow cytometry experiments. Flow cytometry was performed with fluorophore-conjugated antibodies against CD11c, CD11b, Gr-1, B220, NK1.1, CD3e, CD4, CD8a, MHC class II, CD80, CD86, Sca-1, c-kit, CD34, FcγRII/III, and matched isotype controls (Biolegend), CD19, DEC205, CD40, and CD16/CD32, IFN-γ (eBioscience), F4/80 (Invitrogen), CD45.2, CD45.1 (BD Biosciences — Pharmingen), PDCA-1 (Miltenyi Biotec), and EPCR (STEMCELL Technologies). Lineage depletion of BM cells was conducted with tricolor-labeled antibodies against CD3, CD4, CD8a, CD19, Ly-6G, and CD45R and Dynabeads (Invitrogen). For FACS of EPCR-expressing DCs, enriched DCs were stained with the antibodies allophycocyanin–anti-CD11c, phycoerythrin–anti–PDCA-1, and fluorescein isothiocyanate–anti-EPCR, and sorted on a BD Aria Cell Sorter (BD Biosciences). Gates were set with appropriate isotype-matched nonimmune antibody. All cytometric analyses of cell surface markers included a final stain with propidium iodine to exclude dead cells. For detection of intracellular antigens (iNOS, IL-12, IFN-γ), cells were first stained for cell surface markers, followed by permeabilization and fixation using a BD CytoFix/Cytoperm Plus Fixation and Permeabilization Kit with BD Golgi Plug according to the manufacturer's instructions (BD Biosciences), and staining with FITC-labeled antibody flow cytometry was performed on a BD LSRII flow analyzer (BD Biosciences).

Endotoxin challenge and treatment with aPC. LPS (40 mg/kg) was administered via intraperitoneal injection. Bolus doses of 5A-aPC or S360A-aPC (10 μg/mouse; range, 0.4–0.3 μg/g body weight) were administered through intravenous injection into the retro-orbital venous plexus 5–10 minutes after endotoxin challenge. Survival was monitored over a 7-day period following LPS challenge.

BM transplantation. Recipient mice were lethally irradiated with a single dose of 11 Gy from a ^{137}Cs source (Gammacell 40 Extractor irradiator; Best Theratronics) 18–24 hours prior to transplantation. Whole BM was obtained by flushing of the femurs and tibias of donor mice. Cells were collected in RPMI medium (ATCC) with 2% penicillin and streptomycin, filtered using a 70-μM mesh, and counted using an Animal Blood Counter (Scil Vet), and 2.5×10^6 to 5×10^6 cells were injected into the retro-orbital venous plexus of the recipient mice. Marrow recipients were maintained on a regular diet with water containing neomycin sulfate (Sigma-Aldrich), sulfamethoxazole, and trimethoprim (Midwest Veterinary Supply). Six weeks later, hematopoietic reconstitution by donor cells was verified by flow cytometric analysis of CD45.1/45.2 expression in peripheral blood nucleated cells. Wild-type C57BL/6, EPCR^{lo}, and PAR1-null mice expressing CD45.2 received wild-type marrow from B6.SJL mice expressing CD45.1; B6.SJL mice were used as recipients for PAR1- or EPCR-deficient marrow.

For adoptive transfer of sorted DC populations (see above) into mice lacking hematopoietic EPCR expression, cells were washed once in phosphate-buffered saline after sorting and resuspended in RPMI, and 1×10^6 DCs were injected into the retro-orbital venous plexus of the recipient mice 24 hours prior to LPS challenge and aPC treatment. Viability of the transferred cell population was estimated by trypan blue staining of a small sample.

Gene chip analysis. EPCR-expressing DCs were isolated via FACS as described above from 6–10 mice per sample. Total RNA was extracted from the pooled sample using TRIzol reagent (Invitrogen), and 100 ng RNA was amplified using an Affymetrix two-cycle cDNA synthesis kit. CD11c^{hi} cells were collected by FACS from 1 spleen per sample (6 samples per experimental condition), and RNA was prepared from each individual sample. RNA isolated from the 6 available samples was mixed in equal amounts to generate a representative pool for each experimental condition. A total of 100 ng of this pool was amplified as above. Quantitative RT-PCR analysis of 5 differentially expressed genes (*Chi3l3*, *Ngp*, *S100a8*, *Mmp8*, *Procr*) was performed on each of the 6 samples contributing to a pool to verify that mRNA abundance in the pool accurately reflected mRNA abundance in each individual sample. cRNA was synthesized, labeled, fragmented, and hybridized to the array in accordance with the Affymetrix GeneChip expression analysis technical manual. Labeled cRNA was hybridized to GeneChip Mouse Genome 430 Plus 2.0 Arrays interrogating approximately 45,000 transcripts. After hybridization, arrays were washed, stained with PE-conjugated streptavidin (Affymetrix), and scanned. Image data were analyzed with Affymetrix GeneChip operating software (GCOS) and normalized with Robust Multichip Analysis (RMA; www.bioconductor.org/) to determine signal log ratios. The statistical significance of differential gene expression was derived through a 2-tailed Student's *t* test, and false discovery rates (FDRs) were determined with Significance Analysis of Microarrays (SAM) software (http://www-stat.stanford.edu/~tibs/SAM/) as described previously (69). Expression data were analyzed with Microsoft Access using measurements of the difference of log ratios between treatment groups. Ontological pathway analysis was performed with Ingenuity Pathways Analysis (Ingenuity Systems). Hierarchical clustering was conducted with Genesis (http://genome.tugraz.at) (70).

Real-time quantitative PCR. Specific oligonucleotide primers for selected transcripts (Supplemental Table 3) were designed with MacVector 7.0 (MacVector Inc.). Monoplex real-time quantitative RT-PCR was performed using the Applied Biosystems 7500 Real-Time PCR System (Applied Biosystems), a Quantum RNA 18s internal standards kit (Ambion), locus-specific primers (Invitrogen), and QuantiTect SYBR Green PCR Master Mix (QIAGEN) according to the manufacturer's instructions. Synthesis of first-strand cDNA from 0.2–0.5 μg unamplified RNA was accomplished with random hexamers and Superscript II (Invitrogen) according to the manufacturer's instructions. Triplicate locus-specific and 18s PCRs were performed for each gene analyzed in 25-μl reactions that included 2 μl of cDNA and 12.5 μl of 2× SYBR QuantiTect SYBR Green PCR Master Mix possessing 1 μl of locus-specific (10 μM) or 18S-specific competimers (used as a 3:7 ratio of primer/competimer set; each stock set is at 5 μM) and 8.5 μl RNase-free water. Reactions were typically cycled as follows: stage 1, 95°C for 15 minutes; stage 2, 50 cycles at 95°C for 30 seconds, 60°C for 30 seconds, 72°C for 30 seconds and fluorescence acquisition at 75–82°C for 20 seconds (locus specific); stage 3 melt curve at 60–95°C. The cDNA was used for both the locus-specific and the 18s standard curves at undiluted, 1:10, 1:25, 1:50, 1:100, 1:500, and 1:1,000 concentrations. At least 2 points from the standard curve were used as positive controls in each assay. Specificity for all quantitative RT-PCR was verified by both melting curve analysis and 1.5% agarose gel detection of a single product of predicted size. The data were analyzed with Applied Biosystems 7500 software using the cycle threshold for quantification. Relative gene expression data (fold change) between samples was accomplished using the mathematical model described by Pfaffl (71).

Cytokine analysis. Spleens were dissected and lysed in ice-cold PBS containing 0.01% Triton X-100 (Sigma-Aldrich). Lysates were centrifuged at 10,000 *g* for 5 minutes and frozen at –20°C until being assayed for cytokine content or protein content. Total protein content in spleen lysates was assayed using the BCA protein concentration kit (Thermo Scientific). Cytokines were measured using equal protein amounts (solid tissue) or plasma sample volume on the Bio-Plex Pro Mouse Cytokine Assay, 23-Plex Group 1 (Bio-Rad).

Statistics. Unless stated otherwise, all values are expressed as mean ± SD. Differences between all groups were analyzed by 2-tailed Student's *t* test. Survival curves were analyzed by Kaplan-Meier log-rank test. All statistical analyses were performed using the StatView (version 5.0, SAS Institute Inc.) program for Windows.

Acknowledgments

We thank Shaun Coughlin for providing PAR1-deficient mice. This work was supported by National Institute of Allergy and Infectious Diseases grants AI078713 (M.J. Hessner) and AI080557 (H. Weiler); National Heart, Lung and Blood Institute grants HL093388 (H. Weiler), HL31950 (J.H. Griffin), and HL073750 (F.J. Castellino); and by the Ziegler Family Research Chair Foundation (H. Weiler)

Received for publication February 10, 2010, and accepted in revised form June 2, 2010.

Address correspondence to: Hartmut Weiler; Blood Research Institute, BloodCenter of Wisconsin, 8727 Watertown Plank Road, Milwaukee, Wisconsin 53226, USA. Phone: 414.937.3813; Fax: 414.937.6284; E-mail: hartmut.weiler@bcw.edu.

1. Mosnier LO, Zlokovic BV, Griffin JH. The cytoprotective protein C pathway. *Blood*. 2007; 109(8):3161–3172.
2. Xu J, et al. Extracellular histones are major mediators of death in sepsis. *Nat Med*. 2009;15(11):1318–1321.
3. Mosnier LO, et al. Hyperantithrombotic, noncytoprotective Glu149Ala-activated protein C mutant. *Blood*. 2009;113(23):5970–5978.
4. Kerschen EJ, et al. Endotoxemia and sepsis mortality reduction by non-anticoagulant activated protein C. *J Exp Med*. 2007;204(10):2439–2448.
5. Xu J, Ji Y, Zhang X, Drake M, Esmon CT. Endogenous activated protein C signaling is critical to protection of mice from lipopolysaccharide-induced septic shock. *J Thromb Haemost*. 2009;7(5):851–856.
6. Isobe H, et al. Activated protein C prevents endotoxin-induced hypotension in rats by inhibiting excessive production of nitric oxide. *Circulation*. 2001;104(10):1171–1175.
7. Van Sluis GL, et al. Endogenous activated protein C limits cancer cell extravasation through sphingosine-1-phosphate receptor 1-mediated vascular endothelial barrier enhancement. *Blood*. 2009;114(9):1968–1973.

8. Monnet X, Lamia B, Anguel N, Richard C, Bonmarchand G, Teboul JL. Rapid and beneficial hemodynamic effects of activated protein C in septic shock patients. *Intensive Care Med*. 2005; 31(11):1573–1576.
9. Kalil AC, et al. Effects of drotrecogin alfa (activated) in human endotoxemia. *Shock*. 2004;21(3):222–229.
10. Derhaschnig U, Reiter R, Knobl P, Baumgartner M, Keen P, Jilma B. Recombinant human activated protein C (rhAPC; drotrecogin alfa [activated]) has minimal effect on markers of coagulation, fibrinolysis, and inflammation in acute human endotoxemia. *Blood*. 2003;102(6):2093–2098.
11. Niessen F, et al. Endogenous EPCR/aPC-PAR1 signaling prevents inflammation-induced vascular leakage and lethality. *Blood*. 2009;113(12):2859–2866.
12. Andonegui G, et al. Endothelium-derived Toll-like receptor-4 is the key molecule in LPS-induced neutrophil sequestration into lungs. *J Clin Invest*. 2003; 111(7):1011–1020.
13. Nick JA, et al. Recombinant human activated protein C reduces human endotoxin-induced pulmonary inflammation via inhibition of neutrophil chemotaxis. *Blood*. 2004;104(13):3878–3885.
14. Sturn DH, Kaneider NC, Feistritzer C, Djanani A, Fukudome K, Wiedermann CJ. Expression and function of the endothelial protein C receptor in human neutrophils. *Blood*. 2003;102(4):1499–1505.
15. Galligan L, et al. Characterization of protein C receptor expression in monocytes. *Br J Haematol*. 2001;115(2):408–414.
16. Yuksel M, Okajima K, Uchiba M, Horiuchi S, Okabe H. Activated protein C inhibits lipopolysaccharide-induced tumor necrosis factor-alpha production by inhibiting activation of both nuclear factor-kappa B and activator protein-1 in human monocytes. *Thromb Haemost*. 2002;88(2):267–273.
17. Pereira C, Schaer DJ, Bachli EB, Kurrer MO, Schoedon G. Wnt5A/CaMKII signaling contributes to the inflammatory response of macrophages and is a target for the antiinflammatory action of activated protein C and interleukin-10. *Arterioscler Thromb Vasc Biol*. 2008;28(3):504–510.
18. Feistritzer C, Sturn DH, Kaneider NC, Djanani A, Wiedermann CJ. Endothelial protein C receptor-dependent inhibition of human eosinophil chemotaxis by protein C. *J Allergy Clin Immunol*. 2003;112(2):375–381.
19. Joyce DE, Nelson DR, Grinnell BW. Leukocyte and endothelial cell interactions in sepsis: relevance of the protein C pathway. *Crit Care Med*. 2004; 32(5 suppl):S280–S286.
20. Balazs AB, Fabian AJ, Esmon CT, Mulligan RC. Endothelial protein C receptor (CD201) explicitly identifies hematopoietic stem cells in murine bone marrow. *Blood*. 2006;107(6):2317–2321.
21. Challen GA, Boles N, Lin KK, Goodell MA. Mouse hematopoietic stem cell identification and analysis. *Cytometry*. 2009;75(1):14–24.
22. Zheng X, et al. Non-hematopoietic EPCR regulates the coagulation and inflammatory responses during endotoxemia. *J Thromb Haemost*. 2007; 5(7):1394–1400.
23. Shortman K, Naik SH. Steady-state and inflammatory dendritic-cell development. *Nat Rev Immunol*. 2007;7(1):19–30.
24. Spits H, Lanier LL. Natural killer or dendritic: what's in a name? *Immunity*. 2007;26(1):11–16.
25. Blasius AL, Barchet W, Cella M, Colonna M. Development and function of murine B220+CD11c+NK1.1+ cells identify them as a subset of NK cells. *J Exp Med*. 2007;204(11):2561–2568.
26. Chan CW, et al. Interferon-producing killer dendritic cells provide a link between innate and adaptive immunity. *Nat Med*. 2006;12(2):207–213.
27. Vosshenrich CA, et al. CD11cloB220+ interferon-producing killer dendritic cells are activated natural killer cells. *J Exp Med*. 2007;204(11):2569–2578.
28. Vremec D, et al. Production of interferons by dendritic cells, plasmacytoid cells, natural killer cells, and interferon-producing killer dendritic cells. *Blood*. 2007;109(3):1165–1173.
29. Hildner K, et al. Batf3 deficiency reveals a critical role for CD8alpha+ dendritic cells in cytotoxic T cell immunity. *Science*. 2008;322(5904):1097–1100.
30. Shortman K, Heath WR. The CD8+ dendritic cell subset. *Immunol Rev*. 2010;234(1):18–31.
31. Kamath AT, Henri S, Battye F, Tough DF, Shortman K. Developmental kinetics and lifespan of dendritic cells in mouse lymphoid organs. *Blood*. 2002;100(5):1734–1741.
32. Ruedl C, Koebel P, Bachmann M, Hess M, Karjalainen K. Anatomical origin of dendritic cells determines their life span in peripheral lymph nodes. *J Immunol*. 2000;165(9):4910–4916.
33. O'Keeffe M, et al. Mouse plasmacytoid cells: long-lived cells, heterogeneous in surface phenotype and function, that differentiate into CD8(+) dendritic cells only after microbial stimulus. *J Exp Med*. 2002; 196(10):1307–1319.
34. Lopez-Bravo M, Ardavin C. In vivo induction of immune responses to pathogens by conventional dendritic cells. *Immunity*. 2008;29(3):343–351.
35. Villadangos JA, Schnorrer P. Intrinsic and cooperative antigen-presenting functions of dendritic-cell subsets in vivo. *Nat Rev Immunol*. 2007;7(7):543–555.
36. Neuenhahn M, Busch DH. Unique functions of splenic CD8alpha+ dendritic cells during infection with intracellular pathogens. *Immunol Lett*. 2007; 114(2):66–72.
37. Pulendran B, et al. Distinct dendritic cell subsets differentially regulate the class of immune response in vivo. *Proc Natl Acad Sci U S A*. 1999;96(3):1036–1041.
38. Maldonado-Lopez R, et al. CD8alpha+ and CD8alpha- subclasses of dendritic cells direct the development of distinct T helper cells in vivo. *J Exp Med*. 1999;189(3):587–592.
39. Maldonado-Lopez R, Maliszewski C, Urbain J, Moser M. Cytokines regulate the capacity of CD8alpha(+) and CD8alpha(–) dendritic cells to prime Th1/Th2 cells in vivo. *J Immunol*. 2001;167(8):4345–4350.
40. Soares H, et al. A subset of dendritic cells induces CD4+ T cells to produce IFN-gamma by an IL-12-independent but CD70-dependent mechanism in vivo. *J Exp Med*. 2007;204(5):1095–1106.
41. Iyoda T, et al. The CD8+ dendritic cell subset selectively endocytoses dying cells in culture and in vivo. *J Exp Med*. 2002;195(10):1289–1302.
42. Liu K, Iyoda T, Saternus M, Kimura Y, Inaba K, Steinman RM. Immune tolerance after delivery of dying cells to dendritic cells in situ. *J Exp Med*. 2002;196(8):1091–1097.
43. Yamazaki S, et al. CD8+ CD205+ splenic dendritic cells are specialized to induce Foxp3+ regulatory T cells. *J Immunol*. 2008;181(10):6923–6933.
44. Puccetti P, Grohmann U. IDO and regulatory T cells: a role for reverse signalling and non-canonical NF-kappaB activation. *Nat Rev Immunol*. 2007;7(10):817–823.
45. Han MH, et al. Proteomic analysis of active multiple sclerosis lesions reveals therapeutic targets. *Nature*. 2008;451(7182):1076–1081.
46. Gao X, Wang S, Fan Y, Bai H, Yang J, Yang X. CD8+ DC, but Not CD8(–)DC, isolated from BCG-infected mice reduces pathological reactions induced by mycobacterial challenge infection. *PLoS One*. 2010; 5(2):e9281.
47. Bamboat ZM, Ocuin LM, Balachandran VP, Obaid H, Plitas G, Dematteo RP. Conventional DCs reduce liver ischemia/reperfusion injury in mice via IL-10 secretion. *J Clin Invest*. 2010;120(2):559–569.
48. Menezes GB, Lee WY, Zhou H, Waterhouse CC, Cara DC, Kubes P. Selective down-regulation of neutrophil Mac-1 in endotoxemic hepatic microcirculation via IL-10. *J Immunol*. 2009;183(11):7557–7568.
49. Toubai T, et al. Immunization with host-type CD8{alpha}+ dendritic cells reduces experimental acute GVHD in an IL-10-dependent manner. *Blood*. 2010;115(3):724–735.
50. Rodriguez S, et al. Dysfunctional expansion of hematopoietic stem cells and block of myeloid differentiation in lethal sepsis. *Blood*. 2009;114(19):4064–4076.
51. Massberg S, et al. Immunosurveillance by hematopoietic progenitor cells trafficking through blood, lymph, and peripheral tissues. *Cell*. 2007;131(5):994–1008.
52. Nagai Y, et al. Toll-like receptors on hematopoietic progenitor cells stimulate innate immune system replenishment. *Immunity*. 2006;24(6):801–812.
53. Kang SJ, Liang HE, Reizis B, Locksley RM. Regulation of hierarchical clustering and activation of innate immune cells by dendritic cells. *Immunity*. 2008;29(5):819–833.
54. White TC, et al. Protein C supports platelet binding and activation under flow: role of glycoprotein Ib and apolipoprotein E receptor 2. *J Thromb Haemost*. 2008;6(6):995–1002.
55. Yang XV, et al. Activated protein C ligation of ApoER2 (LRP8) causes Dab1-dependent signaling in U937 cells. *Proc Natl Acad Sci U S A*. 2009;106(1):274–279.
56. Hancock WW, et al. Binding of activated protein C to a specific receptor on human mononuclear phagocytes inhibits intracellular calcium signaling and monocyte-dependent proliferative responses. *Transplantation*. 1995;60(12):1525–1532.
57. Niessen F, et al. Dendritic cell PAR1-S1P3 signalling couples coagulation and inflammation. *Nature*. 2008;452(7187):654–658.
58. Shortman K, Liu YJ. Mouse and human dendritic cell subtypes. *Nat Rev Immunol*. 2002;2(3):151–161.
59. Wu L, Liu YJ. Development of dendritic-cell lineages. *Immunity*. 2007;26(6):741–750.
60. Robbins SH, et al. Novel insights into the relationships between dendritic cell subsets in human and mouse revealed by genome-wide expression profiling. *Genome Biol*. 2008;9(1):R17.
61. Caminschi I, et al. The dendritic cell subtype-restricted C-type lectin Clec9A is a target for vaccine enhancement. *Blood*. 2008;112(8):3264–3273.
62. Sancho D, et al. Tumor therapy in mice via antigen targeting to a novel, DC-restricted C-type lectin. *J Clin Invest*. 2008;118(6):2098–2110.
63. Cinel I, Opal SM. Molecular biology of inflammation and sepsis: a primer. *Crit Care Med*. 2009; 37(1):291–304.
64. Rittirsch D, Flierl MA, Ward PA. Harmful molecular mechanisms in sepsis. *Nat Rev Immunol*. 2008; 8(10):776–787.
65. Darrow AL, et al. Biological consequences of thrombin receptor deficiency in mice. *Thromb Haemost*. 1996;76(6):860–866.
66. Connolly AJ, Ishihara H, Kahn ML, Farese RV Jr, Coughlin SR. Role of the thrombin receptor in development and evidence for a second receptor. *Nature*. 1996;381(6582):516–519.
67. Iwaki T, Cruz DT, Martin JA, Castellino FJ. A cardioprotective role for the endothelial protein C receptor in lipopolysaccharide-induced endotoxemia in the mouse. *Blood*. 2005;105(6):2364–2371.
68. Mosnier LO, Gale AJ, Yegneswaran S, Griffin JH. Activated protein C variants with normal cytoprotective but reduced anticoagulant activity. *Blood*. 2004;104(6):1740–1744.
69. Tusher VG, Tibshirani R, Chu G. Significance analysis of microarrays applied to the ionizing radiation response. *Proc Natl Acad Sci U S A*. 2001; 98(9):5116–5121.
70. Sturn A, Quackenbush J, Trajanoski Z. *Genesis*: cluster analysis of microarray data. *Bioinformatics*. 2002;18(1):207–208.
71. Pfaffl MW. A new mathematical model for relative quantification in real-time RT-PCR. *Nucleic Acids Res*. 2001;29(9):e45.